COMPRESSIVE SAMPLING EXPERIMENTS

Carsten Roppel and Martin Danz

Faculty of Electrical Engineering, University of Applied Sciences Schmalkalden
P. O. B. 10 04 52, D-98564 Schmalkalden, Germany
phone: + (49) 3683 688-5110, fax: + (49) 3683 688-5499, email: c.roppel@fh-sm.de, m.danz@stud.fh-sm.de
web: www.fh-schmalkalden.de

ABSTRACT

Compressive sampling theory describes methods to reconstruct signals sampled at sub-Nyquist rates. The theory assumes that the signals are sparse in the frequency domain or in the time domain and requires a random sampling process. This paper describes compressive sampling experiments using a 6 Msps ADC (THS1206) and a C6000 DSP. The sampling instants are defined by pseudorandom binary sequences. The input signals used in our experiments are sine signals and binary phase-shift keying (BPSK) signals.

1. INTRODUCTION

Digital signal processing of analog signals usually assumes that the analog signal is sampled at rate exceeding the Nyquist rate, which is twice the maximum signal frequency. Further processing of the samples often results in a reduced number of samples representing the actual information content. Examples are video cameras, where the samples read from the sensor are compressed to reduce storage space or the bit rate required for transmission, or digital receivers, where after demodulation, equalization and matched filtering the signal is downsampled to one sample per symbol.

Compressive sampling or compressive sensing (CS) allows to recover a signal from far fewer samples, thus combining sampling and compression [1]. CS assumes that the signal is sparse when expressed in a suitable domain, i. e. it can be described with a small number of parameters. Consider for example the time and the frequency domain. A signal is sparse in the frequency domain, if its frequency transform has only a few nonzero coefficients, while the location and amplitude of the nonzero coefficients is unknown. However, CS can also be applied to signals that are sparse in the time domain [2], and it is not restricted to time and frequency domain representations [1].

One way to obtain the samples representing the signal is random sampling, i. e. nonuniform sampling, at an average rate below the Nyquist rate. While it is possible to simulate such a system, we decided to perform some simple hardware experiments where signals are randomly sampled and further processed. In simulations (e. g. with Matlab), samples are generated in software. It is sometimes not clear, if a practical sampling scheme exists which allows to obtain the same samples from a real-world signal.

Some hardware experiments using special and powerful hardware are reported in the literature [3], [4]. The goal of our simple experiments using standard hardware is to provide a platform for students to learn the concepts behind CS not only based on numerical simulations.

2. COMPRESSIVE SENSING

2.1 Signal Description

Consider a discrete-time, real-valued signal $x(n)$ of finite length. This can be viewed as a $N \times 1$ column vector $\mathbf{x}$ with elements x_i, $i = 1, \ldots, N$. Using the notation introduced in [5], the signal $\mathbf{x}$ can be expressed as

$$\mathbf{x} = \mathbf{\Psi}\, \mathbf{s}\,, \tag{1}$$

where $\mathbf{\Psi}$ is a $N \times N$ orthonormal basis matrix and $\mathbf{s}$ is the coefficient vector, a $N \times 1$ column vector. $\mathbf{x}$ and $\mathbf{s}$ are equivalent representations of the signal in different domains. Here, we concentrate on the time and the frequency domain. Well-known examples for such representations are the discrete Fourier transform (DFT) and the discrete cosine transform (DCT). Consider an N-point DFT in the usual form

$$\begin{aligned} S_{DFT}(k) &= \sum_{n=0}^{N-1} x(n) \exp\left(-\mathrm{j}\, 2\pi\, n\, k / N\right) \\ x(n) &= \frac{1}{N} \sum_{k=0}^{N-1} S_{DFT}(k) \exp\left(\mathrm{j}\, 2\pi\, n\, k / N\right) \end{aligned} \tag{2}$$

with $k = 0, \ldots, N-1$ and $n = 0, \ldots, N-1$, respectively. Rearranging the equations gives

$$\begin{aligned} S_{DFT}(k) &= \sqrt{N} \sum_{n=1}^{N} x(n) \frac{1}{\sqrt{N}} \exp\left(-\mathrm{j}\, 2\pi\, (n-1)\,(k-1) / N\right) \\ x(n) &= \frac{1}{\sqrt{N}} \sum_{k=1}^{N} S_{DFT}(k) \frac{1}{\sqrt{N}} \exp\left(\mathrm{j}\, 2\pi\, (n-1)\,(k-1) / N\right) \end{aligned} \tag{3}$$

with $k = 1, \ldots, N$ and $n = 1, \ldots, N$, respectively. A comparison with Eq. (1) shows that the elements of the matrix $\mathbf{\Psi}$ are

$$\Psi_{n,k} = \frac{1}{\sqrt{N}} \exp\left(\mathrm{j}\, 2\pi\, (n-1)\,(k-1) / N\right) \tag{4}$$

and the elements of vector $\mathbf{s}$ are $S_{DFT}(k)$, $k = 1, \ldots, N$. In case of the DCT, the elements of $\mathbf{\Psi}$ are real and given by

$$\Psi_{n,k} = w(k)\cos\left(\frac{\pi(2n-1)(k-1)}{2N}\right) \quad (5)$$

with $k = 1, \ldots, N$ and $n = 1, \ldots, N$ and $w(k) = 1/\sqrt{N}$ for $k = 1$ and $w(k) = 2/\sqrt{N}$ for $k = 2, \ldots, N$.

If **s** has K nonzero and $N - K$ zero coefficients, the signal **x** is K-sparse. In general **x** is compressible if the coefficient vector has a few large elements, while the remaining elements are small.

In traditional data compression a signal is sampled at a rate above the Nyquist rate and a compression algorithm is applied. Consider for example transform coding, where N samples are acquired. Next, the coefficient vector $\mathbf{s} = \mathbf{\Psi}^H \mathbf{x}$ is computed, where $\mathbf{\Psi}^H$ is the Hermitian transpose (conjugate transpose) of $\mathbf{\Psi}$. The values and positions of the K largest coefficients are encoded to obtain a compressed signal description. In contrast to this, compressed sensing directly acquires the compressed signal. In general, $M < N$ measurements are obtained, from which **x** is recovered by means of a suitable reconstruction algorithm.

2.2 Sub-Nyquist Sampling

A simple way to obtain M measurements from the signal **x** in the time domain is to select M out of N samples, where the average sampling rate is below the Nyquist rate. If the samples are selected randomly, the representation in the time domain and the frequency domain are orthogonal with high probability. This property of the measurement process is referred to as incoherence [1].

In a practical system, the M samples are taken from the analog signal $x(t)$, where a nonuniform sampling clock defines the sampling instants. Nonuniform sampling schemes have a long history as a research subject, see e. g. [6], where Poisson sampling, random skipping of samples and jittered sampling are discussed.

Completely random sampling instants imply problems with regard to the minimum spacing of sampling instants allowed by the analog-to-digital converter (ADC) and further signal processing. A systematic method of generating suitable sampling patterns is not known. Here, we consider the random selection of sampling instants from a uniform sampling grid. The sampling pattern is defined by a pseudo-random binary sequence (PRBS). Because of the periodic nature of the PRBS, the number of sampling instants per period defines the number of samples per block for further processing.

Nonuniform sampling is not the only method to obtain M measurements. Another way for example is to compute M linear combinations of the N elements x_i, where the elements are weighted with random variables generated from a Gaussian probability density function [5].

2.3 Signal Reconstruction

Now consider a measurement of the signal **x** which results in the vector **y** having $M < N$ elements, representing the M measurements. This is described by

$$\mathbf{y} = \mathbf{\Phi}\,\mathbf{x}, \quad (6)$$

with the $M \times N$ measurement matrix $\mathbf{\Phi}$. In the case of random sampling, $\mathbf{\Phi}$ is composed of M rows of a $N \times N$ identity matrix. This corresponds to selecting M out of N samples of **x** as described in Section 2.2. Substituting Eq. (1) we have

$$\mathbf{y} = \mathbf{\Phi}\,\mathbf{\Psi}\,\mathbf{s} = \mathbf{\Theta}\,\mathbf{s}, \quad (7)$$

where the $M \times N$ matrix $\mathbf{\Theta}$ is called the sensing matrix. Eq. (7) is an underdetermined system of M equations with N unknowns, the N elements of **s**. However, if **s** is sparse, i. e. if it contains only a few nonzero elements, CS theory shows that it is possible to find a solution if $\mathbf{\Theta}$ satisfies the restricted isometry property [1]. The solution is given by a vector $\hat{\mathbf{s}}$ that minimizes the l_1 norm

$$\|\mathbf{s}'\|_1 = \sum_{i=1}^{N} |s_i'|. \quad (8)$$

That is from all vectors **s'** satisfying $\mathbf{\Theta}\,\mathbf{s}' = \mathbf{y}$ we select the one with minimum l_1 norm. Once we know $\hat{\mathbf{s}}$, we can reconstruct the signal

$$\mathbf{x} \approx \mathbf{\Psi}\,\hat{\mathbf{s}}. \quad (9)$$

Finding $\hat{\mathbf{s}}$ is an optimization problem which can be solved in a linear program. For our experiments we used an implementation described in [7].

Analog-to-Information receivers directly extract parameters from a signal based on CS theory, avoiding the computational complexity associated with signal reconstruction as described above. This approach could be useful in RF receivers for signal demodulation. Among the receiver architectures proposed we find the random demodulator (RD) [8], the random-modulator pre-integrator (RMPI) [9] and the modulated wideband converter (MWC) [3]. In all these architectures there is an analog preprocessing stage, where typically the signal is multiplied with a random sequence. The output of the multiplier is integrated or lowpass filtered and sampled uniformly with a low sampling rate.

3. NONUNIFORM SAMPLING EXPERIMENTS

3.1 Hardware Setup

For the experiments the THS1206 ADC [10] is used as the sampling device. The signal and the nonuniform sampling clock are generated with a two-channel arbitrary waveform generator (Rohde & Schwarz SMBV100A). In this way various signals and nonuniform sampling schemes can be tested. The THS1206 is connected to a C6713 DSK (Figure 1).

The internal sampling rate of the signal generator is set to 16 MHz. A sampling clock pulse is composed of eight successive ones followed by eight zeros. Thus the

maximum frequency of the sampling clock is 1 MHz. The maximum value is limited by the THS1206 to 6 MHz.

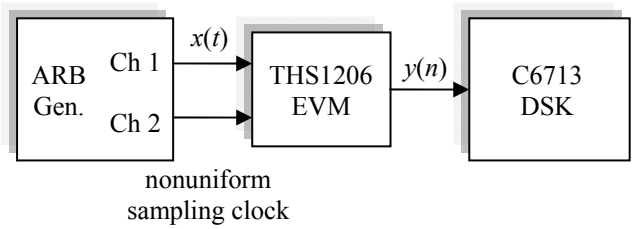

Figure 1 – Hardware setup with arbitrary waveform generator (ARB Gen.), THS1206 EVM and C6713 DSK.

The sampling instants are defined by pseudorandom binary sequences (PRBS). We used a PRBS127 specified by the generator polynomial $g(x) = x^7 + x^3 + 1$, which repeats after $L = 127$ values. It contains 64 ones corresponding to 64 sampling instants, and the average sampling rate is 503.94 kHz. The second PRBS used is a PRBS1023 defined by the generator polynomial $g(x) = x^{10} + x^3 + 1$, which repeats after $L = 1023$ values and contains 512 ones. For the PRBS1023 sequence the average sampling rate is 500.49 kHz.

3.2 Test Signals

The signal $x(t)$ generated by the signal generator is either a 300 kHz sine wave or a BPSK (binary phase-shift keying) signal. The BPSK signal has a carrier frequency $f_c = 300$ kHz, a symbol rate of $r_s = 125$ kbaud and uses a raised cosine pulse shaping filter with a roll-off factor of $\alpha = 0.5$. Figure 2 shows the BPSK signal together with the first sampling clock pulses defined by the PRBS1023 sequence.

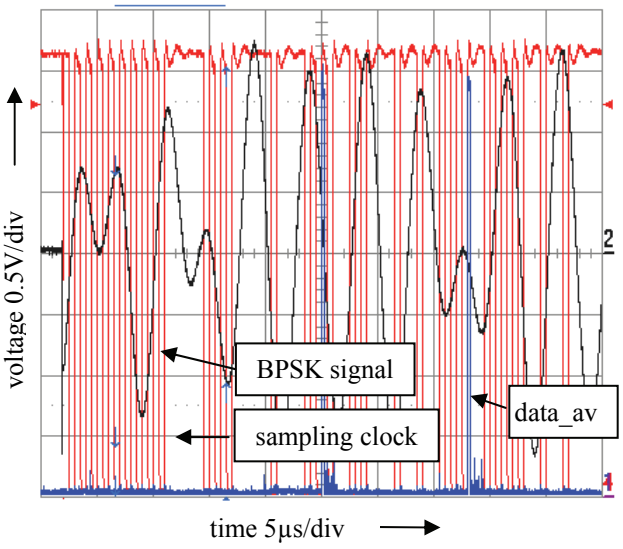

Figure 2 – Oscillogram showing the BPSK signal, the PRBS1023 sampling clock and the data available (data_av) of the THS1206 ADC.

Also shown in Figure 2 is the data available signal data_av generated by the ADC. The THS1206 has an internal FIFO, which is programmed to set data_av high when 8 samples are stored in the FIFO. This signal interrupts the DSP and the samples are transferred via direct memory access (DMA) into the DSP memory. The first data_av pulse in Figure 2 is delayed because of the THS1206 internal pipeline structure. In our experiments the device was able to sample the signal exactly although the sampling period was not uniform.

Figure 3 shows the further processing of the samples. After reading the samples from the ping-pong buffer a buffer is filled with 32000 samples. These samples are transferred to the host computer and are further processed with Matlab.

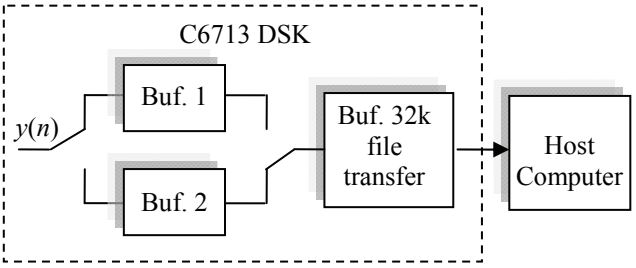

Figure 3 – Transfer of samples from the THS1206 via C6713 DSK to the host computer.

4. EXPERIMENTAL EVALUATION

4.1 Signal Reconstruction

The signal reconstruction is done in Matlab. Each measurement results in 32000 samples. After importing the data into Matlab, we first checked if the samples are in accordance with the ideal samples taken from the reference signal at the sampling instants defined by the nonuniform sampling pattern.

$\boldsymbol{\Psi}$ is a $N \times N$ DCT matrix with elements defined by Eq. (5), and $\boldsymbol{\Theta}$ is a $M \times N$ matrix and consists of M rows of $\boldsymbol{\Psi}$ as described in Section 2.3. For the PRBS127 sampling sequence, $N = 127$ and $M = 64$, while for the the PRBS1023 sequence we have $N = 1023$ and $M = 512$. The 32000 samples available are divided into blocks of M samples to obtain $\mathbf{y}$. It is important to synchronize $\mathbf{y}$ with the PRBS sequence, i. e. the M samples correspond to one period of the PRBS sequence. For each block, $\hat{\mathbf{s}}$ and $\mathbf{x}$ according to Eq. (9) are calculated.

4.2 Sine Signal

The first test signal is a 300 kHz sine wave sampled with the PRBS127 sequence. Figure 4 shows a good match of the reference samples generated with Matlab and the samples acquired with the THS1206 ADC. Figure 5 shows the estimated DCT $\hat{\mathbf{s}}$ and the reconstructed signal $\mathbf{x}$ for one block. Finally, Figure 6 shows the power spectrum of the reconstructed signal obtained from 30 blocks or 3819 samples. The 300 kHz component is clearly visible, however the reconstructed signal shows much more out-of-band spectral components compared to the reference signal.

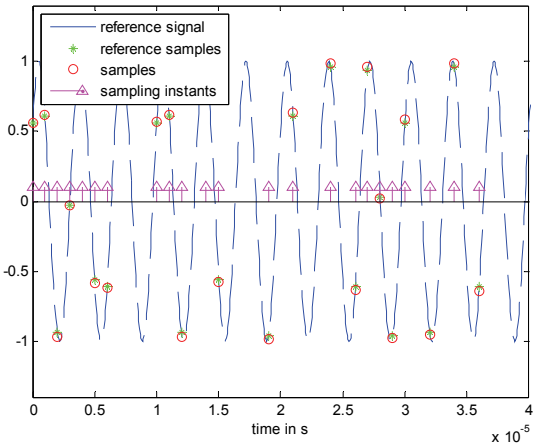

Figure 4 – Matlab-generated 300 kHz sine wave reference signal and reference samples, and samples acquired with THS1206 ADC. Vertical arrows indicate the sampling instants defined by the PRBS127 sequence.

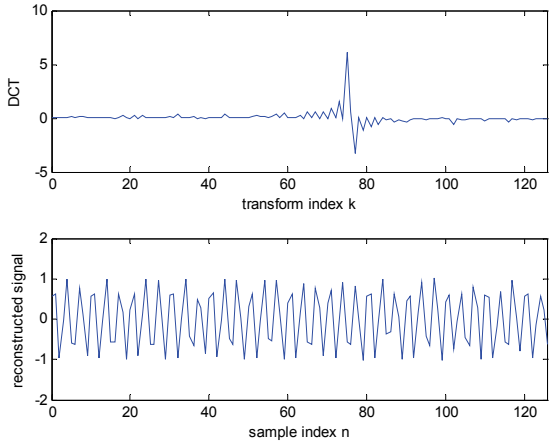

Figure 5 – 127-point DCT (top) and reconstructed signal in the time domain (bottom).

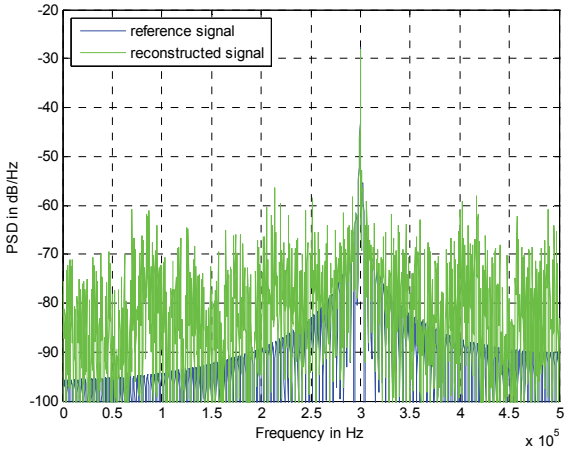

Figure 6 – Power spectral density obtained from the 300 kHz sine wave reference signal and the reconstructed signal. The reconstructed signal is composed of 30 blocks each having 127 samples.

4.3 BPSK Signal

The next test signal is a BPSK signal centered at $f_c = 300$ kHz having a bandwidth $B = (1+\alpha)\, r_s = 187.5$ kHz. The sampling sequence is the PRBS1023 sequence. Again, the samples acquired by the ADC are in excellent agreement with the Matlab generated reference samples. Figure 7 shows the power spectrum of the reconstructed signal obtained from 30 blocks or 30690 samples. The signal spectrum is clearly recovered, but similar to Figure 6 the spectrum of the reconstructed signal shows higher out-of-band components when compared to the reference signal.

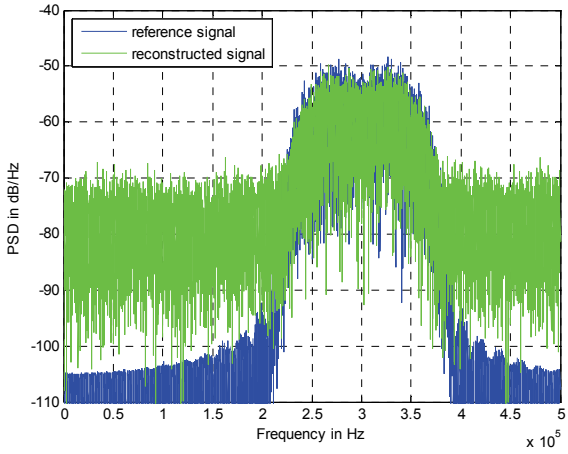

Figure 7 – Power spectral density obtained from the BPSK reference signal and the reconstructed signal. The reconstructed signal is composed of 30 blocks each having 1023 samples.

Figure 8 shows the scatter plot of the demodulated signal. The Figure shows 112 symbols obtained from one block. Although we can clearly see the BPSK signal constellation, there is a significant spreading around the ideal constellation. To exclude effects from the sampling device, we compare the signal reconstructed from the THS1206 samples and the signal reconstructed from the reference samples. The difference in the symbol values is caused by the difference of the ADC samples and the reference samples. But both scatter plots show similar spreading, which is a result of the reconstruction process.

We also compared the PRBS127 with the PRBS1023 sampling sequence. When processing the same number of samples in both cases, the scatter plots showed a similar variance around the ideal signal constellation, revealing no fundamental difference in the performance of the two sampling schemes.

Because our BPSK signal occupies a significant bandwidth in the first Nyquist zone, we also tested BPSK signals with a smaller bandwidth. Figure 9 shows the spectrum of two BPSK signals, one centered at 130 kHz and the other centered at 300 kHz. The symbol rate is reduced by a factor of 4 to $r_s = 31.25$ kbaud, resulting in a bandwidth of $B = 46.875$ kHz.

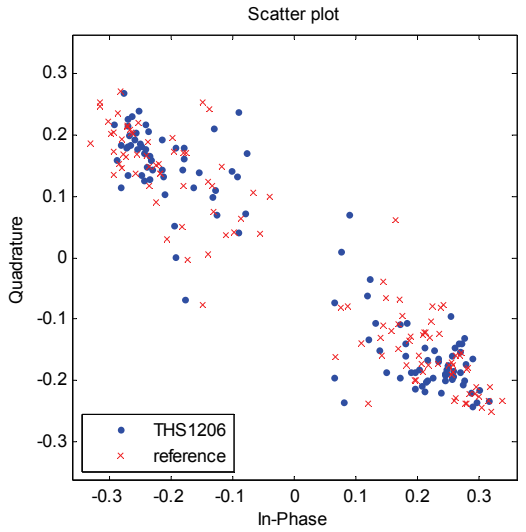

Figure 8 – Scatter plot (112 symbols) of the reconstructed BPSK signal (B = 187.5 kHz) and the reference signal after demodulation.

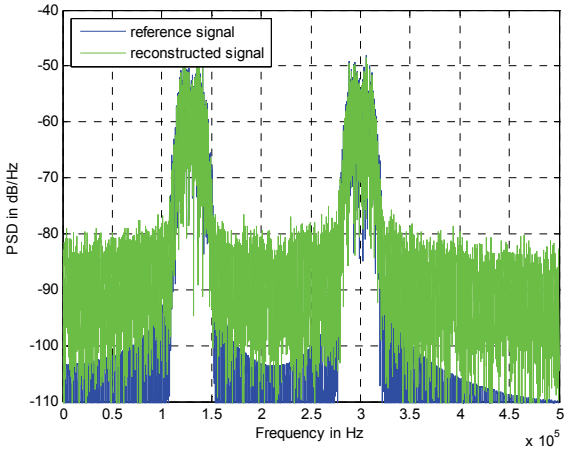

Figure 9 – Power spectral density obtained from two BPSK signals with carrier frequencies 130 kHz and 300 kHz. The reconstructed signal is composed of 30 blocks each having 1023 samples.

Figure 10 shows the scatterplot of the demodulated signal at f_c = 300 kHz. The Figure shows 951 symbols obtained from 30 blocks of the reconstructed signal. Even though the plot shows much more symbols the variation is significantly less when compared to Figure 8. This is because the signal reconstruction algorithm works much better when the total occupied bandwidth is smaller.

5. CONCLUSIONS

The experiments showed that signal reconstruction is possible from samples obtained from a THS1206 ADC driven by a random sampling clock with an average sampling rate below the Nyquist rate. For practical reasons periodic sampling sequences defined by a PRBS are preferred. The recovery algorithm requires synchronization with the PRBS.

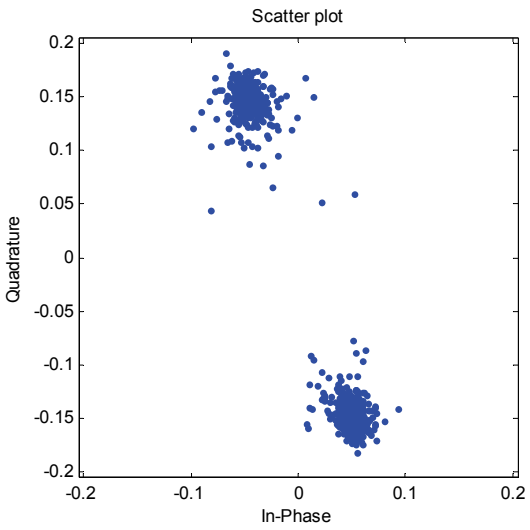

Figure 10 – Scatter plot (951 symbols) of the reconstructed BPSK at 300 kHz (B = 46.875 kHz) signal after demodulation.

REFERENCES

[1] E. J. Candès, M. B. Wakin, "An Introduction To Compressive Sampling", *IEEE Signal Processing Mag.*, pp. 21-30, March 2008.

[2] T. Blu, P.-L. Dragotti, M. Vetterli, P. Marziliano, L. Coulot, "Sparse Sampling of Signal Innovations", *IEEE Signal Processing Mag.*, pp. 31-40, March 2008.

[3] M. Mishali, Y. C. Eldar, "Sub-Nyquist Sampling", *IEEE Signal Processing Mag.*, pp. 98-124, November 2011.

[4] E. Nakamura, "Compressive Samplers for RF Environments", *IEEE Communications Mag.*, pp. 124-129, October 2013.

[5] R. G. Baraniuk, "Compressive Sensing", *IEEE Signal Processing Mag.*, pp. 118-120, 124, July 2007.

[6] F. J. Beutler, "Alias-Free Randomly Timed Sampling of Stochastic Processes", *IEEE Trans. Inform. Theory*, vol. IT-16, no. 2, pp. 147-152, March 1970.

[7] E. J. Candés, J, Romberg, "l_1-MAGIC: Recovery of Sparse Signals via Convex Programming", October 2005, available at users.ece.gatech.edu/~justin/l1magic.

[8] J. A. Tropp, J. N. Laska, M. F. Duarte, J. K. Romberg, and R. G. Baraniuk, "Beyond Nyquist: Efficient sampling of sparse bandlimited signals", *IEEE Trans. Inform. Theory*, vol. 56, no. 1, pp. 520–544, Jan. 2010.

[9] J. Yoo *et al.*, "A Compressed Sensing Parameter Extraction Platform for Radar Pulse Signal Acquisition", *IEEE J. Emerging and Sel. Topics in Circuits and Sys.*, vol. 2, no. 3, Sept 2012, pp. 626–38.

[10] THS1206 12-Bit 6 MSPS Simultaneous Sampling Analog-to-Digital-Converter Data Sheet, SLAS217H, Texas Instruments, 2003.